# 2

# Modelling Coastal Sediment Transport for Harbour Planning: Selected Case Studies

Vincent Leys[1] and Ryan P. Mulligan[2]
*[1]CBCL Limited Consulting Engineers, Halifax NS*
*[2]East Carolina University, Greenville NC*
*[1]Canada*
*[2]USA*

## 1. Introduction

During the planning phase of coastal development projects, it is often necessary to determine potential sedimentation and erosion rates. This is particularly relevant at harbours where dredged channels are proposed, and accurate dredging projections are crucial for economic feasibility analyses. In addition, new structures that interfere with the natural processes may have major impacts on the adjacent shoreline.

In this chapter we consider a range of approaches for evaluating sediment transport for harbour planning studies (section 2), and present two detailed cases from Atlantic Canada. The sites described are representative of very different coastal environments. They include Saint John Harbour (section 3), a uniquely dynamic estuary on the Bay of Fundy with huge tides, a very large river outflow and significant sedimentation of silt and clay presenting various navigation and dredging challenges. The other site described is located on the sandy North coast of Prince Edward Island at Darnley Inlet, an exposed area where tides, storms and sea level rise are continuously reshaping the shoreline and navigation channels (section 4).

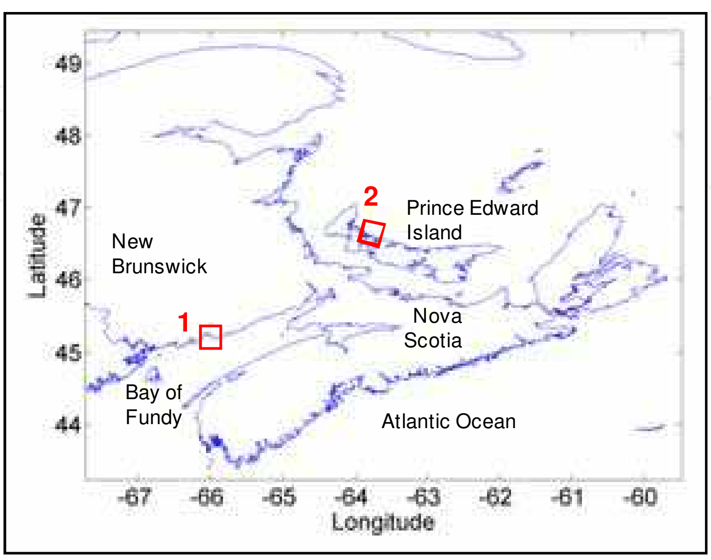


Fig. 1. Location of Saint John Harbour (1) , and Darnley Inlet (2) in Atlantic Canada

To put the case studies in perspective, a brief summary of approaches for evaluating coastal sediment transport processes is provided. The approaches include preliminary site investigations and data collection, basic sediment transport theory, and a range of numerical modelling techniques that can be applied to determine sediment erosion, transport and deposition.

## 2. Approaches for evaluating sediment transport

Engineering studies in natural environments have site specific conditions that require a unique approach to each problem. Therefore some or all of the following methods may need to be applied in order to determine the impacts of harbour structures on the sedimentological environment. Some adverse impacts may include interruption of the net wave-induced longshore transport causing downdrift erosion, scour at the base of breakwaters or jetties, silting-up of harbour basins requiring repeated dredging, increased agitation due to reflected waves, or increased currents through harbour openings. After the construction of new structures, sediment flows will adjust to a new equilibrium, typically over a timescale of years. Thus the effects of human-intervention on the coastal environment are not immediately obvious and coastal developments require careful planning.

**Site investigations**

Every harbour has a unique combination of structures, environmental forcing conditions, sediment sources and supply. Site investigations should include:

• Acquisition of bathymetry, water level, wind, wave and sediment properties information;

• Observation of shoreline features to identify erosional/ depositional landforms;

• Examination of aerial photographs, which gives a larger scale view of the area and may allow other landforms to be identified. Analysing a sequence of historical aerial photography is the first (and oftentimes the most accurate) method to assess sediment processes and determine rates of change.

As a brief example, sediment flux at Arisaig, on Nova Scotia's North shore is dominated by wave-driven longshore transport supplied by sandy cliffs. The original harbour facing the direction of longshore transport became a natural sand trap. A new breakwater and extension of existing rock structures were recently considered. Some important aspects considered in the design process included impacts of episodic major storms, seasonal and annual climate variability, changes in water levels, and changes in up-drift shoreline use that affect the sediment supply from beaches, rivers or cliffs.


Fig. 2. Arisaig Harbour, Nova Scotia, 2003.

**Shoreline contour models**

Shoreline contour models simulate the evolution of one bathymetric contour (generally the shoreline at mean water level). They typically assume uniform grain size, beach profile shape and depth of closure (the seaward depth at which repeatedly surveyed profiles intersect). These models, developed for straight sandy coastlines, predate the full morphological models discussed next. However, within limitations, these models are very effective for long-term predictions of shoreline change when coastal structures are introduced or modified. As an example, consider the one-dimensional diffusion equation:

$$\frac{\partial y}{\partial t} - D\frac{\partial^2 y}{\partial x^2} = 0 \qquad (1)$$

where y is the cross-shore coordinate, x is the alongshore coordinate, t is time and D (longshore diffusivity) is related to the sediment transport rate, beach profile shape and wave conditions. The equation can be solved analytically (Pelnard-Considere 1956, Dean 2002) and used to model the progressive shoreline evolution from an initially straight shoreline, assuming steady-state wave and sediment conditions and one structure perpendicular to the coast. As shown in Fig. 3, accretion against the up-drift side of the structure increases with time until the contour intersects the end of the structure, at which time bypassing begins.

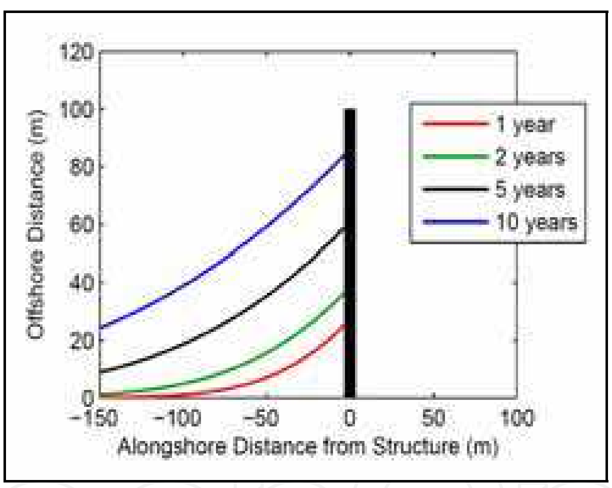


Fig. 3. Example sediment accretion along a groin estimated by a 1-D shoreline change model.

More sophisticated 1D models have been developed with the capability of simulating the beach response to the introduction of different coastal structures such as groins, detached breakwaters or seawalls. The shoreline models LITPACK (DHI 2008) and GENESIS (Generalized Model for Simulating Shoreline Change, (Gravens et al 1991)) simulate long-term averaged shoreline change produced by spatial and temporal differences in wave parameters and longshore sediment transport. The NLINE model (Dabees and Kamphuis, 2000) simulates beach evolution for multiple contour lines.

**Hydrodynamic and morphological models**

Morphodynamic models rely on numerical routines that explicitly predict the wave and hydrodynamic forcing, and sediment transport in two or three dimensions. The hydrodynamic models numerically solve the fluid momentum and continuity equations in order to predict water level changes, circulation and transport driven by winds, waves, tides, river discharge or density forcing. Some examples include Delft3D (Lesser et al, 2004), the Regional Ocean Modeling System (ROMS, Shchepetkin and McWilliams, 2005), Coupled MIKE21 (DHI 2009) and FVCOM (Chen et al, 2006). An example using Delft3D is shown on Fig. 4. Examples using MIKE by DHI are presented in the detailed case studies following this section. Each uses different numerical techniques, includes different features and operates on different types of computational grids (i.e. rectangular, curvilinear or unstructured).

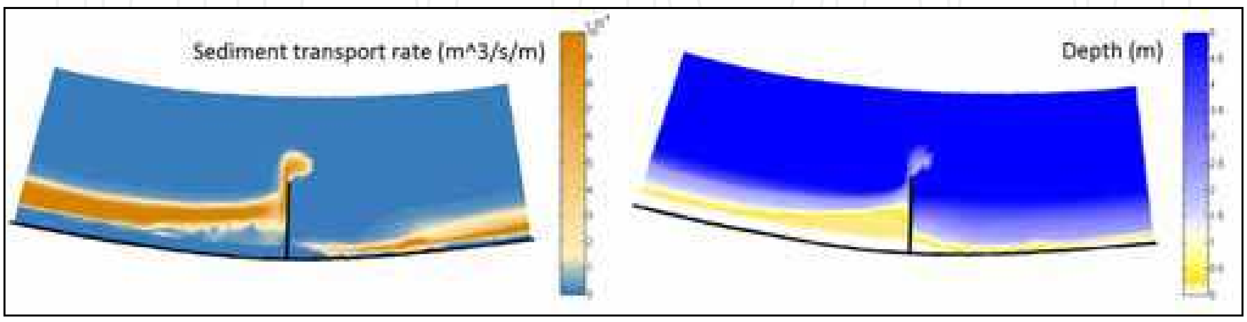


Fig. 4. Example of longshore sediment transport rate and resulting bathymetry along a sandy beach one year after introducing a groin, predicted using the Delft3D model.

Separately, a wave model is employed to predict wave transformation. The wave model is either a phase-averaging (spectral) or a phase-resolving (Boussinesq) model. The wave and hydrodynamic models typically operate on different timescales but are coupled such that they communicate at specified time steps. The wave model is used to propagate wave energy throughout the model domain, and predict changes to the wave energy distribution by refraction, diffraction, wind generation, non-linear energy transfers, dissipation (e.g. white-capping, bottom friction, and breaking) and interaction with currents. Examples of phase-averaged models include the SWAN model (Simulating Waves Nearshore, Booij et al, 1999), and MIKE21 SW (DHI 2009). Examples of phase-resolving models include CGWAVE (Demirbilek & Panchang 1998) and MIKE21 BW (DHI 2009). Phase-averaged models are typically more computationally efficient, since larger spatial resolution, larger time steps and simpler physics are used. Phase-resolving models are typically better at handling reflection and diffraction which become important processes near coastal structures and inside harbour basins.

The morphological models are coupled with the hydrodynamic models by including sediment equations to predict bottom shear stresses and track sediment concentrations through the model domain. Morphological models typically use a bed shear stress formulation in the form:

$$\tau_b = \rho C_D u_b |u_b| \tag{2}$$

where ρ is water density, $u_b$ is the is the horizontal velocity above the bed, and $C_D$ is a drag coefficient. The drag coefficient is proportional to von Karman's constant, the thickness of the bed layer, and the roughness length of the bed. The bed roughness length is used to parameterize sub-grid scale roughness features including bedforms and individual grains. Other sediment routines parameterize sediment processes, such as roughness in the bottom boundary layer, bedload and suspended-load transport, particle fall velocity and flocculation, with different formulations for cohesive and non-cohesive sediments. Sediment is eroded, transported, deposited and the bed morphology evolves with time. Examples are the Community Sediment Transport Model (CSTM, Warner et al, 2008), Delft3D and MIKE 3.

## 3. Saint John Harbour

**Background**

The marine physical environment of Saint John Harbour is very complex and dynamic. Key parameters such as water level, density and flow are highly variable in time and space due to the interaction of large semi-diurnal tides (of maximum range 8.9m) with strong freshwater discharge from the Saint John River, one of the largest rivers in Eastern Canada. The large tides are due to the fact that the Gulf of Maine-Bay of Fundy system is close to being in resonance with the semi-diurnal forcing from the North Atlantic (Greenberg 1990). The unusual characteristic of Saint John Harbour is that the large tides are being countered by particularly strong river outflow. The river discharges into the Harbour across a 200 m wide ridge and then through a narrow rock gorge (Fig. 6), creating spectacular rapids that

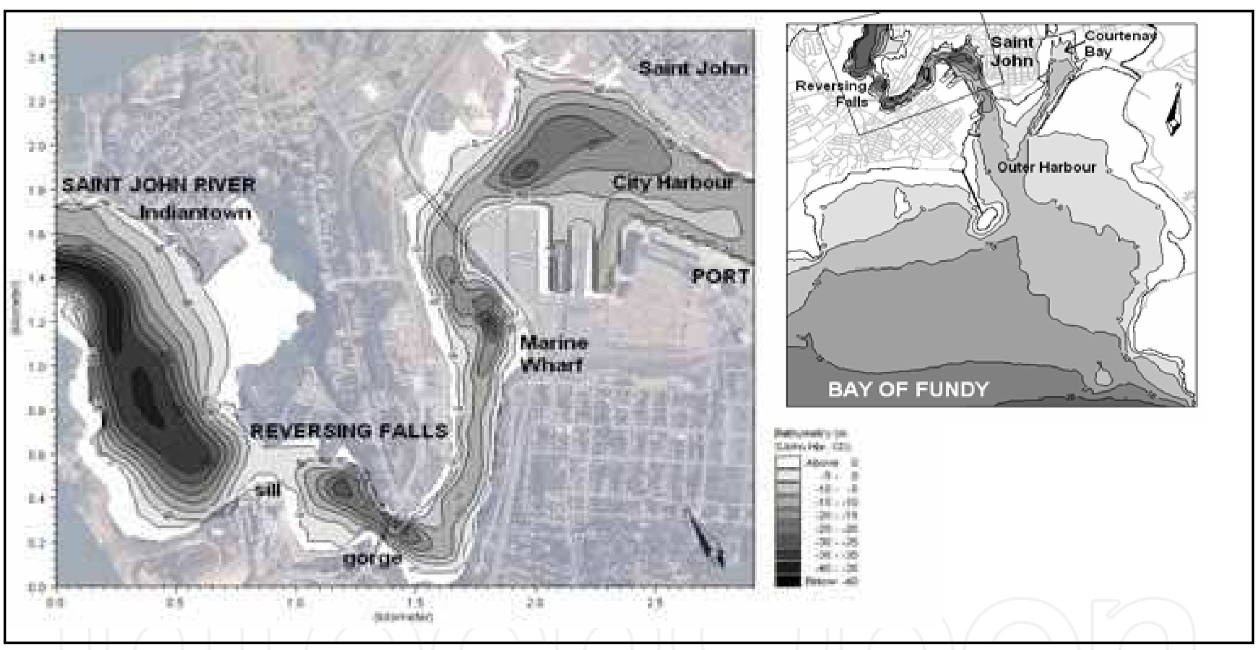


Fig. 5. Study area and bathymetry: Reversing Falls and adjacent channel reaches (left), Saint John Harbour on the Bay of Fundy (right).

Fig. 6. The Reversing Falls gorge at ebb tide, looking Northeast (16/ 11/ 2006).

reverse direction with the tides. The Reversing Falls only allow a relatively small volume discharge in and out over a tidal cycle. This hydraulic control causes a significant difference in the water levels on either side of the constriction and locally strong currents alternating in direction.

**Dredging records**

Downstream of the Falls, the Port of Saint John requires maintenance dredging of fine sediments settling along piers and in navigation channels. Target dredging areas for the Port of Saint John are shown in Fig. 7, along with summary grain size distributions. The dredging areas include channels in the Outer Harbour and Courtenay Bay, and deepwater berths in the City Harbour.

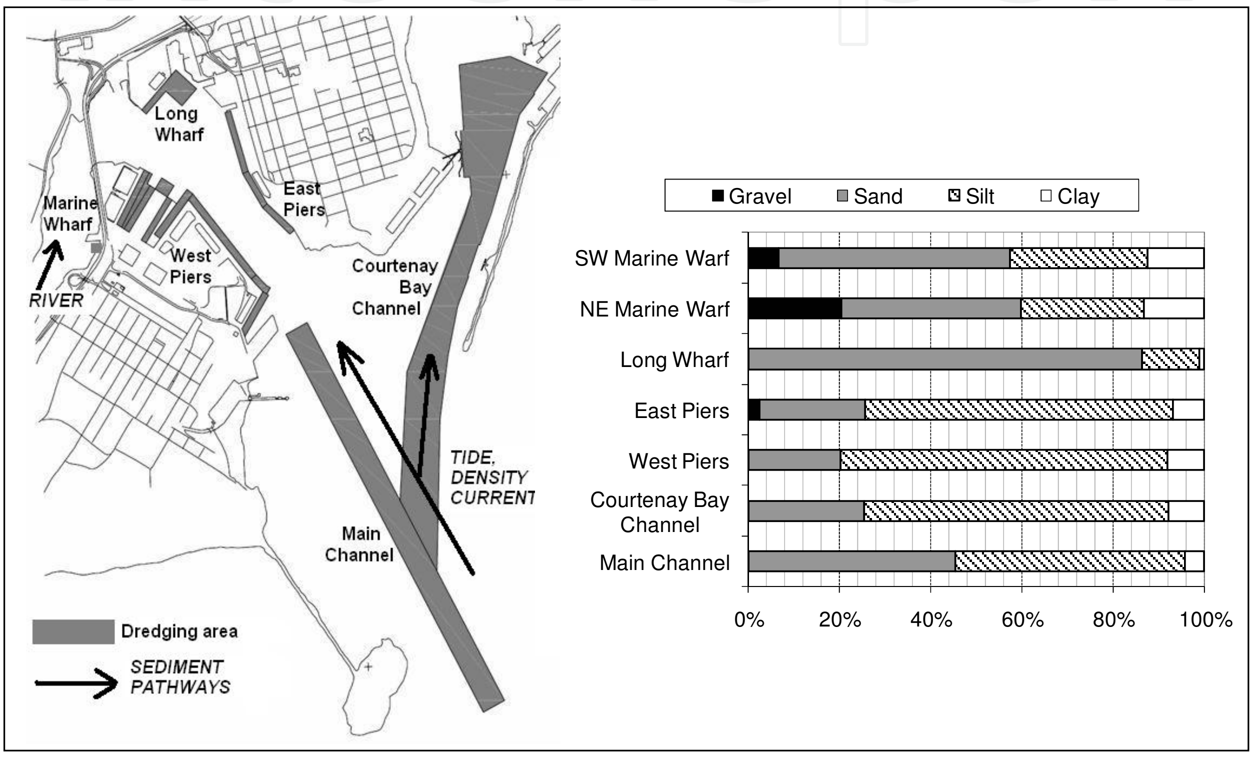


Fig. 7. Saint John Harbour dredging areas and grain size distributions (2006 data – source: Saint John Port Authority).

Measured dredging volumes represent the best available 'benchmark' data for estimating a mean annual sedimentation rate. However the extrapolation from scow-measured dredging volumes to sedimentation rate carries considerable uncertainty due to the bulking factor. The bulking factor is the ratio of dredged volume immediately after deposition in the scow, to the in-situ volume of the same mass of material. As a general rule of thumb, the smaller the grain size, the larger the bulking factor: sand can bulk up 1.0 to 1.2, silt 1.2 to 1.8 and clay 1.5 to 3.0 (USACE 2004). In addition, actual dredging areas vary from year to year, and may be less than target areas, possibly by a factor of 2 or 3. Ranges for sedimentation rates have been developed based on dredging records weighed with the above uncertainty factors. The calculated ranges represent averages in time and space, which could be exceeded in any given year or location. It is estimated that the sedimentation rates range from 0.2 to 1m/year, the higher end of the bracket applying to the deepwater berths in the City Harbour. The dredging records show considerable variability in the quantities from year to year, resulting in the wide range.

**Description of sedimentation processes**

The ample sediment supply combined with the hydrodynamic regime cause extensive sedimentation in dredging areas. These areas tend to decelerate sediment-bearing flows, and represent a departure from a natural equilibrium state where sedimentation is balanced by erosion. The primary local sediment sources include the River, the seabed of the Bay of Fundy and eroding coastlines. An extensive review of harbour sedimentation (or 'siltation') mechanisms is provided by Winterwerp (2005). Sediment transport modelling must resolve the following three major site-specific processes:

1. *Density currents* - The density difference between tidally-driven salt water inflow and freshwater river outflow causes an estuarine circulation pattern characterized by a mean seaward surface flow and a mean up-harbour bottom flow. The residual dense bottom flows carry silt that is deposited in the more stagnant areas. Sedimentation in dredging areas is due in most part to marine silt carried into the Harbour by the bottom density current (Neu 1960). Notably, yearly variations in river outflow and suspended concentrations in the river do not correspond to variations in the measured dredged quantities.
2. *Tidal exchange* - Water within a harbour basin is replaced by freshwater from the river water on the ebb tide, and then by saline water on the flood tide (with the exception of the near-surface where a layer of freshwater persists). This efficient and continuous exchange mechanism is caused both by the very large tidal range and by the large river discharge. Settling then occurs wherever weaker currents allow. The sedimentation rate depends on a complex array of variables including tidal prism (volume entering the harbour), trapping efficiency, suspended sediment concentrations, dry bed density and settling rates vs. local currents. Of these variables, settling rate probably has the highest variability and influence.
3. *Horizontal eddy exchange* - During peak flows, suspended sediments are transported in the lee of protruding wharf structures due to energetic residual eddies shed from the structures. Deposition occurs where weak currents and high settling rates allow.

**Hydrodynamic modelling**

The Danish Hydraulic Institute's MIKE3 finite-volume model was implemented to better understand flow patterns and sediment transport in the harbour, and to assist in the evaluation of maintenance dredging requirements for future harbour facilities. The hydrodynamic module solves the hydrostatic momentum and continuity equations, including the effects of turbulence and variable density, and the conservation equations for salinity in three dimensions together with the equation of state of sea water relating the local density to salinity, temperature and pressure. The model also features a coupled advection-diffusion algorithm to model the evolution of suspended sediment concentrations, which serve as input to the sediment transport module.

The model domain consists of an unstructured mesh of 2,590 triangular elements in each horizontal layer. In the vertical dimension, the model was set-up using up to 23 layers in the deepest areas. The upper three layers were defined as compressible 'sigma' layers following the oscillations in water level. Below a fixed depth of 1m below low tide, the model used 20 strictly horizontal 2m thick layers to better resolve the density stratification. The model domain (Fig. 8) was set-up to include all dredging areas, with its upstream boundary 500m downstream of the Reversing Falls. The upstream boundary conditions for this model (water level, salinity and suspended sediment concentrations) were obtained by extracting data from a calibrated, non-hydrostatic and higher-resolution MIKE3 hydrodynamic model of the Reversing Falls channel developed for a previous study (Leys 2007). At the Bay of Fundy boundary, tidal predictions were used as well as time-series of vertical salinity and suspended sediment concentrations constructed from field observations by Neu (1960).

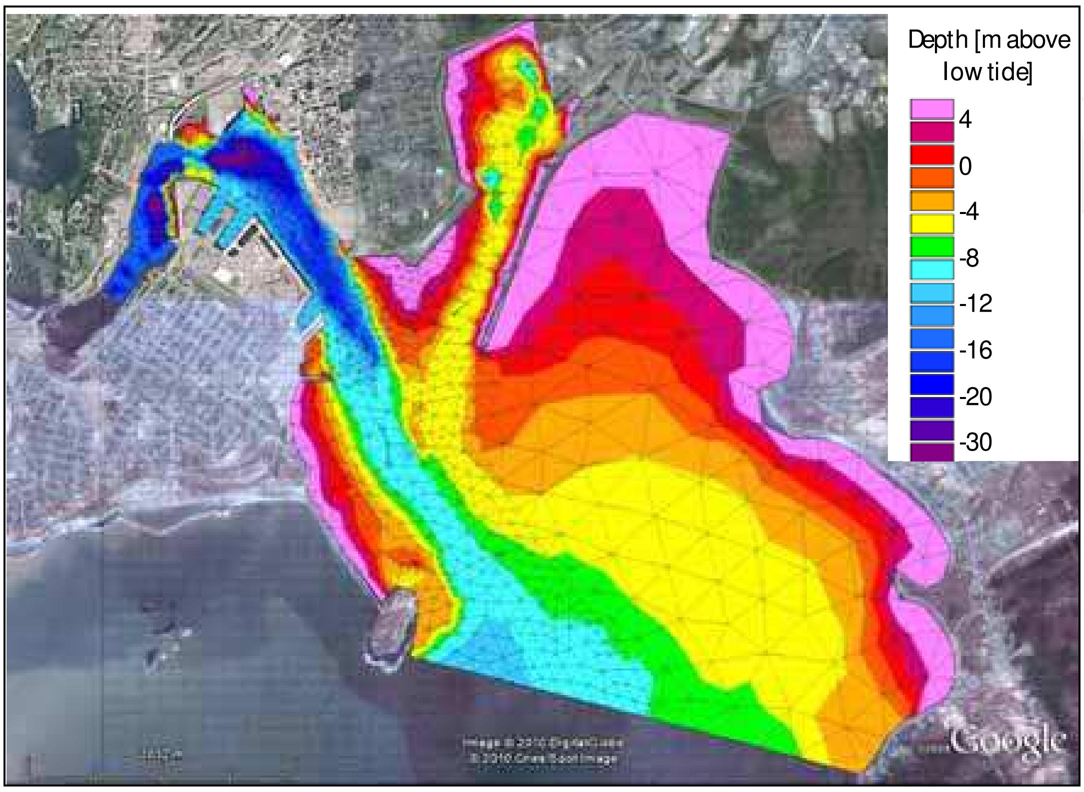


Fig. 8. Saint John Harbour Model mesh.

**Vertical profiles**

The evolution of vertical profiles for key model variables over a tidal cycle is shown on Fig. 9 at the intersection of the Main Channel and Courtenay Bay channel (see Fig. 7). The three dimensional circulation patterns are evidenced by salinity and Total Suspended Sediment (TSS) fields over a mean tidal cycle. During flood tide and at high tide, the bottom layer of denser, saline and sediment-laden tidal water extends into the channel and flows opposite the seaward surface current. On the ebb and low tide, saltwater is gradually replaced from surface to bottom by freshwater from the river which carries coarser and lower sediment content. The model results are consistent with field data, but show a stratified phase of shorter duration.

**Residual current patterns**

Residual bottom current patterns (i.e. averaged over a tidal cycle) are important as they govern the movement of the sediment-laden bottom layer. Residual currents over a mean tidal cycle during summer conditions are presented in Fig. 10. The results indicate that the mean currents along the bottom move in the up-harbour direction. The modelled bottom density current in the City Harbour and Courtenay Bay Channel is approximately 0.1m/ s, slightly less than residual currents calculated from summer field measurement by Neu (1960). Modelled near-surface residual currents for summer conditions correspond well to past measurements, with values in the order of 0.3 to 0.4 m/ s in the City Harbour.

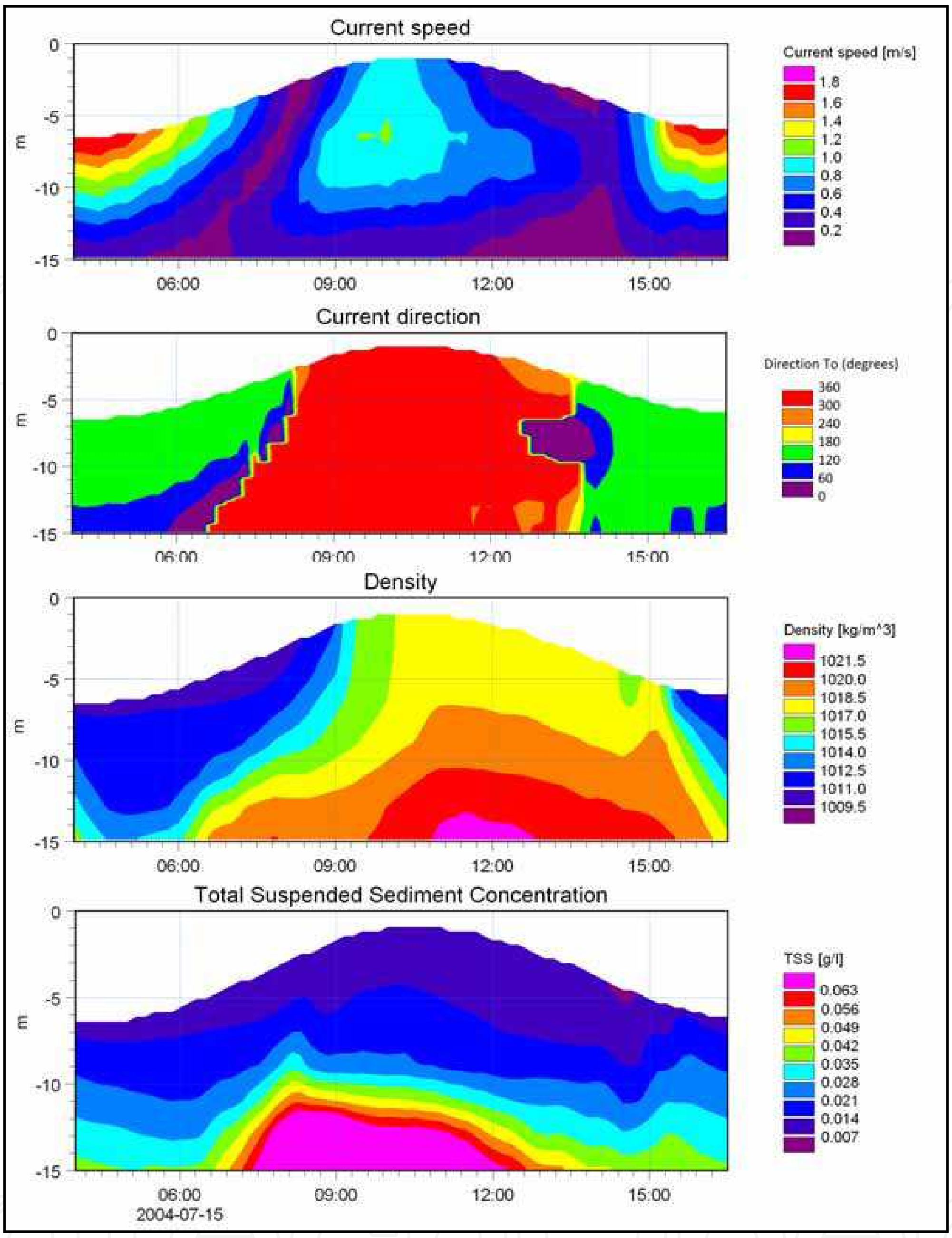


Fig. 9. Vertical profiles of model fields over one tidal cycle at the intersection of the Main Channel and Courtenay Bay channel.

**Sediment transport model**

The DHI MIKE3 Mud Transport Model calculates sediment transport of fine material in estuaries and coastal areas, for dredging and sedimentation studies. This model was used to simulate the erosion, transport and deposition of fine grained and cohesive material under the action of river, tidal and density currents calculated by the hydrodynamic model. Values for sediment parameters were adjusted within realistic ranges based on field data (suspended sediment concentrations and dredging records). Two fine sediment fractions were included in the model, which form the bulk of sediment deposits in dredged areas: sandy silt and clayey silt. The critical shear stress for deposition and settling velocity were treated as calibration parameters and the values adopted are listed in Table 1. At the open

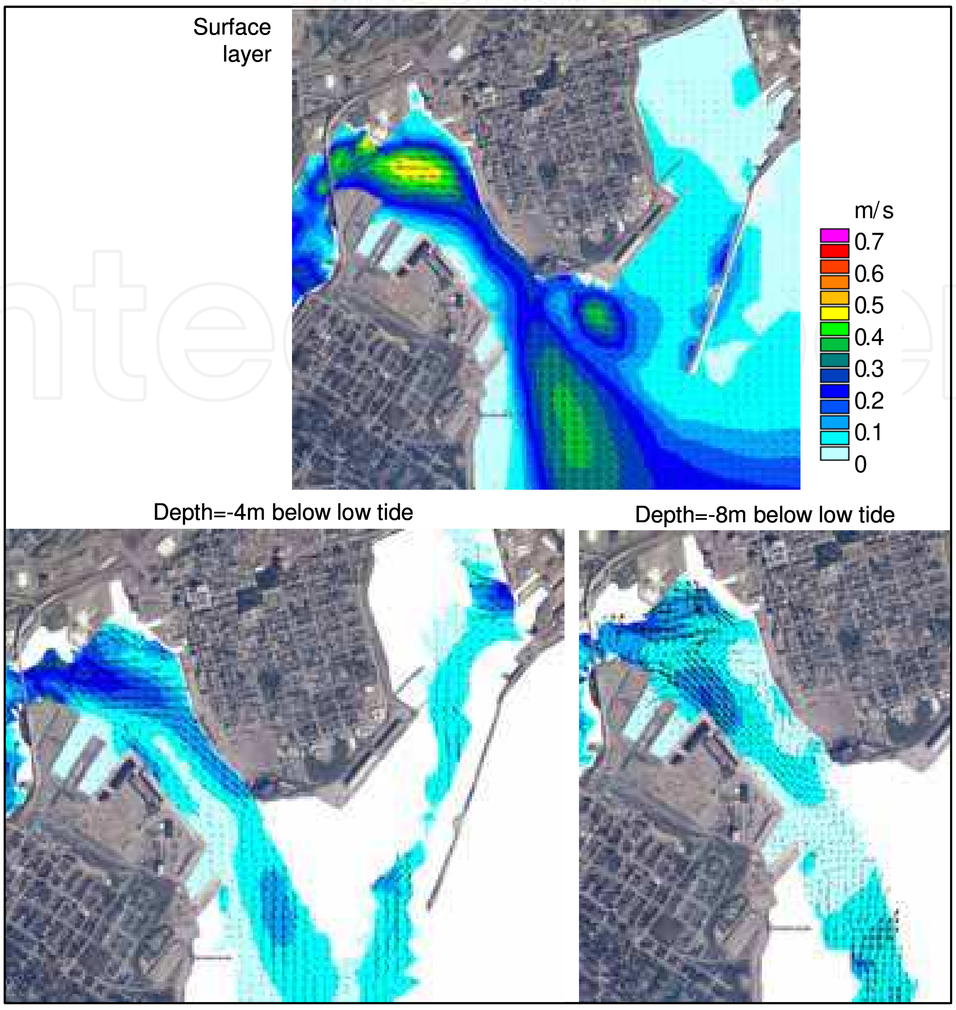


Fig. 10. Modelled residual flow patterns for summer conditions showing seaward surface flow from river (top panel) and up-harbour density current at the bottom (bottom panels).

boundaries, time-series of depth-varying suspended sediment concentrations were developed based on summer data from Neu (1960) and recent additional sampling (Leys 2007).

| Parameter | Fraction 1 Clayey Silt | Fraction 2 Sandy Silt | Comments |
|---|---|---|---|
| Representative grain size [mm] | 0.005 | 0.05 | For reference – not actually used in computations |
| Critical shear stress for deposition [N/ m2] | 0.01 | 0.09 | At each model time step, erosion or deposition algorithms are triggered if the bed stress is respectively above or below critical value |
| Settling velocity [mm/ s] | 0.1 | 1 | For fine sediment the settling velocity can vary by several orders of magnitude. Flocculation, which generally starts at concentrations higher than observed in typical conditions, was not included. |

Table 1. Input sediment characteristics for MIKE3 MT model.

The model accuracy can only be as good as the accuracy of dredging records used in the calibration process. Based on the Port dredging records, the estimated error range from the modelled sedimentation rates is -50% to +100% (i.e., in any given year the actual value could be twice as low or twice as high as predicted). Under existing conditions the finer fraction (clayey silt) deposits primarily in the calmer areas, i.e., Courtenay Bay and within rectangular mooring basins (Fig. 11). The coarser fraction (sandy silt) causes more deposition in the main channel, and there is still a significant amount that settles alongside piers. A comparison between deposition quantities for the two fractions over the entire model area indicates approximately 6 times more mass deposition for the coarser sandy silt fraction. This indicates that a large proportion of the fine fraction modelled remains in suspension in the more energetic areas.

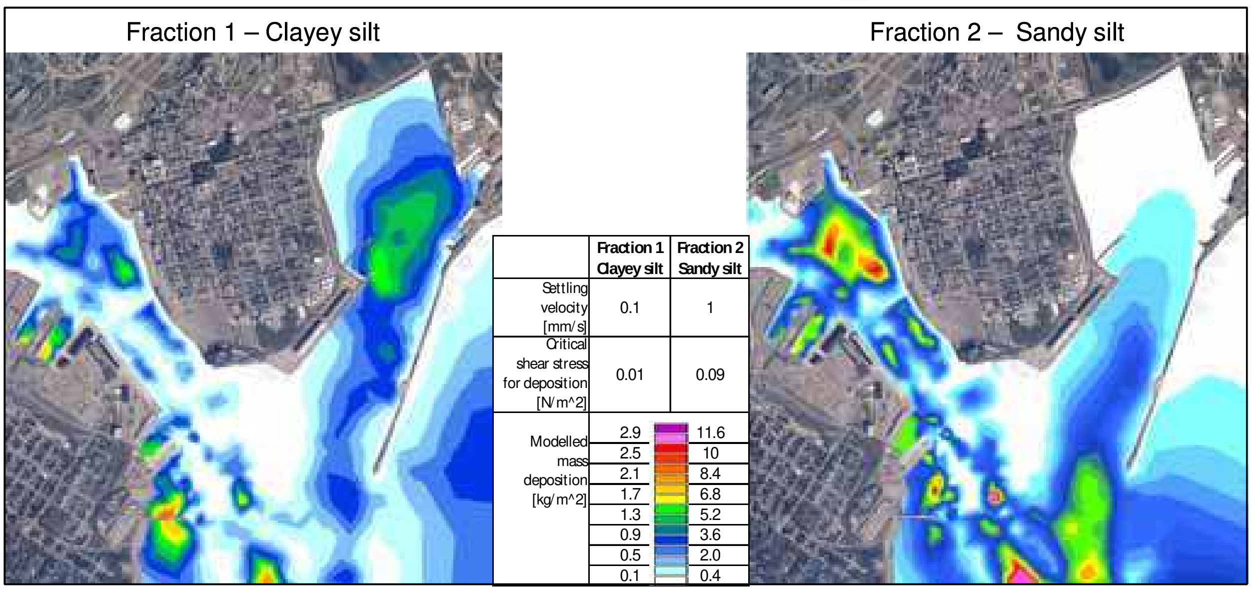


| | Fraction 1 Clayey silt | Fraction 2 Sandy silt |
|---|---|---|
| Settling velocity [mm/s] | 0.1 | 1 |
| Critical shear stress for deposition [N/m^2] | 0.01 | 0.09 |
| Modelled mass deposition [kg/m^2] | 2.9 | 11.6 |
| | 2.5 | 10 |
| | 2.1 | 8.4 |
| | 1.7 | 6.8 |
| | 1.3 | 5.2 |
| | 0.9 | 3.6 |
| | 0.5 | 2.0 |
| | 0.1 | 0.4 |

Fig. 11. Modelled mass deposition for two sediment fractions after 15 days.

The large difference in mass deposition between the two fractions is reduced when applying dry bed density to convert mass deposition into volume and determine the sedimentation rate. For a given mass accumulation calculated from settling, the dry bed density dictates the corresponding volume accumulation and therefore sedimentation rate.

Values were selected based on moisture contents of surficial sediment samples varying from 40% to 80% for freshly deposited silt. For example, a given mass deposition of clayey silt in Courtenay Bay (where dry bed density was assumed low at 200 kg/m$^3$) will result in a larger thickness than the same mass deposition of sandy silt in the centre of main channel where dry bed density is likely higher (assumed at 1000 kg/m$^3$).

Modelled sedimentation rates were extrapolated to a yearly basis based on a 2-week model run, which provides patterns that are generally consistent with annual dredging records for Port areas (Fig. 12). Sedimentation rates peak within man-made indentations in the shoreline, and in sections of the dredged channels where currents are lower such as the Courtenay Bay Channel along the eastern breakwater.

The model also helped understand why observed sedimentation rates in the Port were uncorrelated with the duration and the intensity of the spring freshet. It was previously thought that the source of the deposited sediment (River or Bay of Fundy) could influence the seasonal variations in sedimentation rates. Measurements from Neu (1960) indicate the suspended loads from the River during the spring freshet are much greater, on the order of 50 mg/l (comparable to typical bottom tidal loads) as opposed to 10 mg/l or less in the summer. Observations from the Port Authority indicate that yearly variations in river outflow do not correspond to observed variations in the dredged quantities. In an attempt to quantify the source region, modelled suspended sediment was divided into two fractions based on origin: the River or Harbour boundary. The results indicate that tidal currents account for more than 50% of the transport to and deposition within the harbour. Typical spring freshet conditions were also investigated. Conceptual model runs were conducted for non-reversing flow conditions (when river levels remain above high tide) and with increased suspended loads from the river boundary. Overall sedimentation rates were found to be in the same order of magnitude as during tidal, reversing flow conditions. Under these conditions the absence of prevailing tidal loads is compensated by the increase in river loads and settling. Continuous non-reversing flow conditions only occur during typically 2 weeks in the spring. Therefore, the influence of the spring freshet on harbour sedimentation is likely limited.

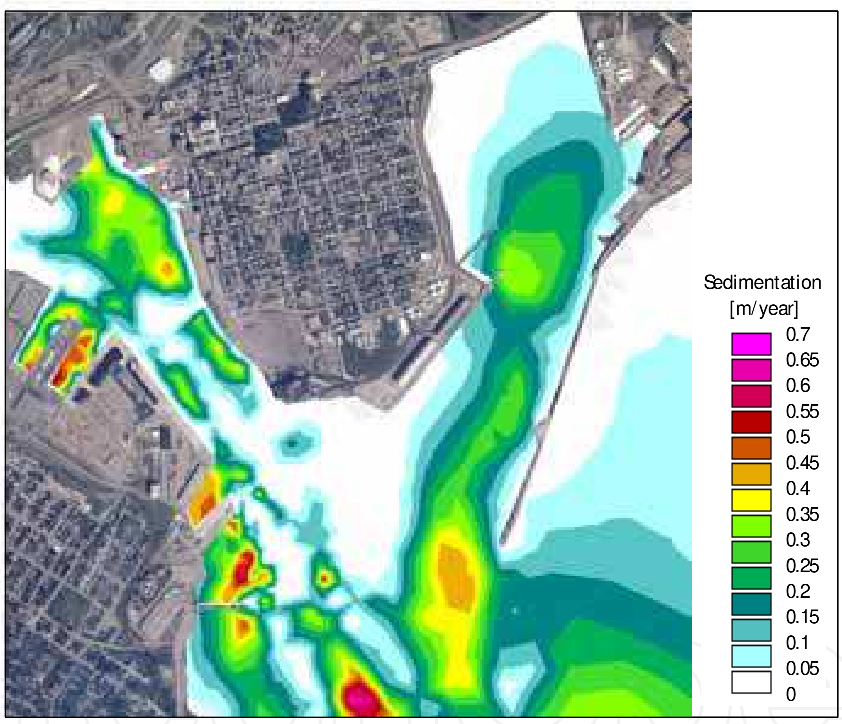


Fig. 12. Modelled annual sedimentation rate.

The model is presently being used to optimize modifications to selected piers or mooring basins, taking into account challenges presented by current velocities and sedimentation. As demonstrated, accumulation rates in new dredging areas can be estimated, within a certain error range depending on the reliability of dredging records. Predicting yearly variations in sedimentation over dredging areas of the Port would also be useful for Port users, but would require a vast amount of additional field data and modelling efforts.
Saint John Harbour provides a good example for fine suspended sediment transport driven by tidal and density flows within a man-made port. The next case study describes a very different site where coarser sand transport prevails, driven by waves and tidal currents at a natural inlet without coastal structures.

## 4. Darnley inlet

Darnley inlet is located on the sandy North Shore of Prince Edward Island. The coast is formed of dunes, barrier islands and tidal inlets, and it is particularly sensitive to storms and sea level rise (Forbes et al 2004, McCulloch et al 2002). At various tidal inlets, dynamic coastal processes occurring on very different time-scales (tides, storms, long-term sea level rise) play an active role in sediment transport, presenting short-term navigation challenges and causing a long-term evolution in the geomorphology.

Malpeque Harbour is located within Darnley Basin (Fig 13). The long winding channel from the harbour exits through the inlet between two sand spits, then becomes considerably shallower as it fans out over a shallow sand bar 500 to 600m from the inlet throat. The bar is referred to as an 'ebb shoal' for the greater influence of the ebb tide on sediment transport. The ebb shoal represents the primary bypassing route for westward sediment transport, and bi-annual dredging is required at the ebb shoal to ensure navigational safety.

Considerations of the tidal prism (the volume exchanged over a tidal cycle) and longshore sediment transport have helped to understand historical changes in the inlet location and dune build-up. In-depth modelling analyses were conducted with a morphological model to better understand sedimentation at the ebb shoal, and to predict morphologic responses to channel-training structures such as jetties.

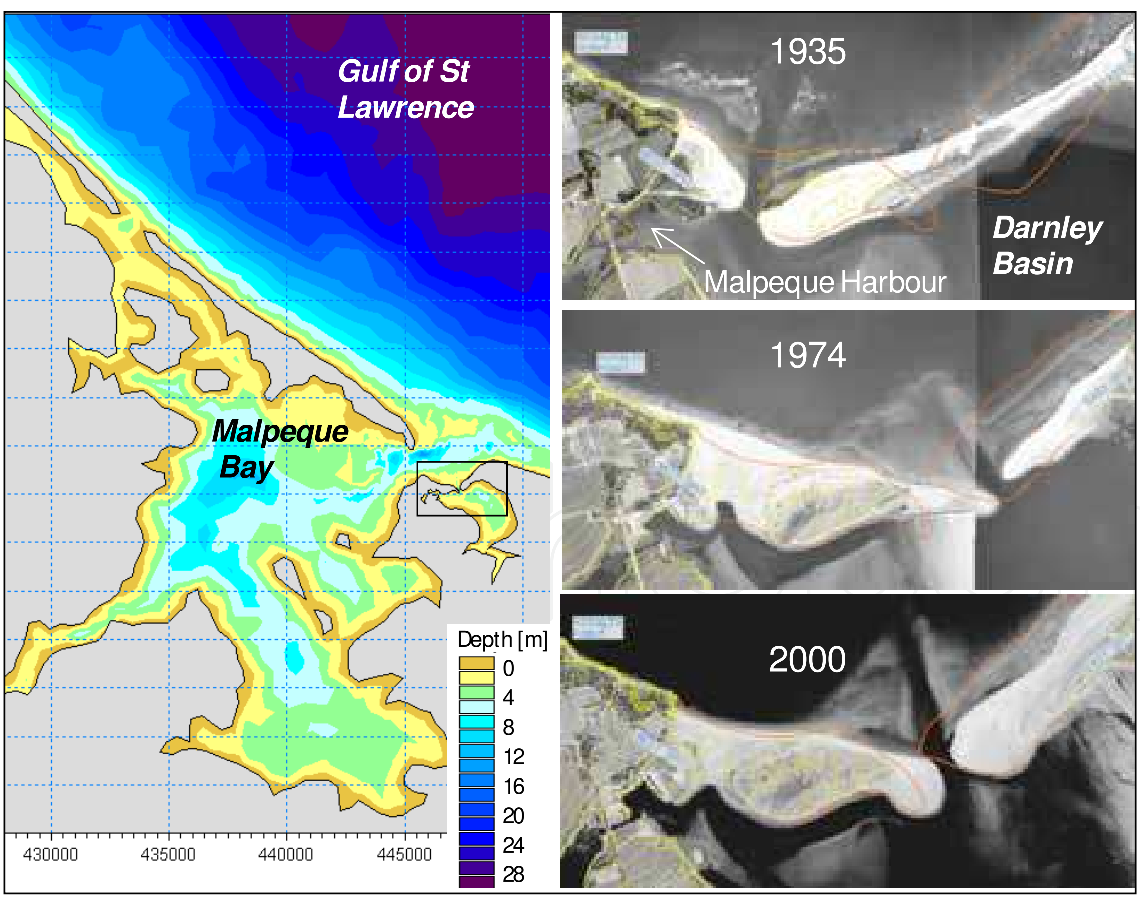


Fig. 13. Site location (left) and historical air photos at Darnley Inlet (right) showing beach evolution, inlet migration and locations of the East and West Spits. The 2008 shoreline is represented with the orange line.

**Historical evolution**

Darnley Inlet is an interesting example of an unstable natural inlet, where the inlet throat has moved considerably over the past century. In the first half of the 20th century, the inlet was located at the base of the present West spit (Fig. 13). The old inlet closed in the 1960's while the new inlet opened through the East spit. Due to westward net longshore transport decreasing toward the inlet, the East spit is accreting and the inlet location is presently migrating westward at a rate of about 14m/ year.

**Tidal hydrodynamics**

The local tides are of mixed type, i.e. with diurnal and semi-diurnal influence. This creates asymmetries in the hydrodynamic regime (e.g. ebb or flood dominance) that have implications on sediment transport.

A hydrodynamic model of the inlet was developed using DHI MIKE21 to estimate key inlet variables that influence sediment dynamics, including tidal prism and ebb or flood dominance. MIKE21 is a two-dimensional, finite-volume model solving the momentum and continuity equations over a finite volume mesh (Fig. 14) to simulate hydrodynamic circulation.

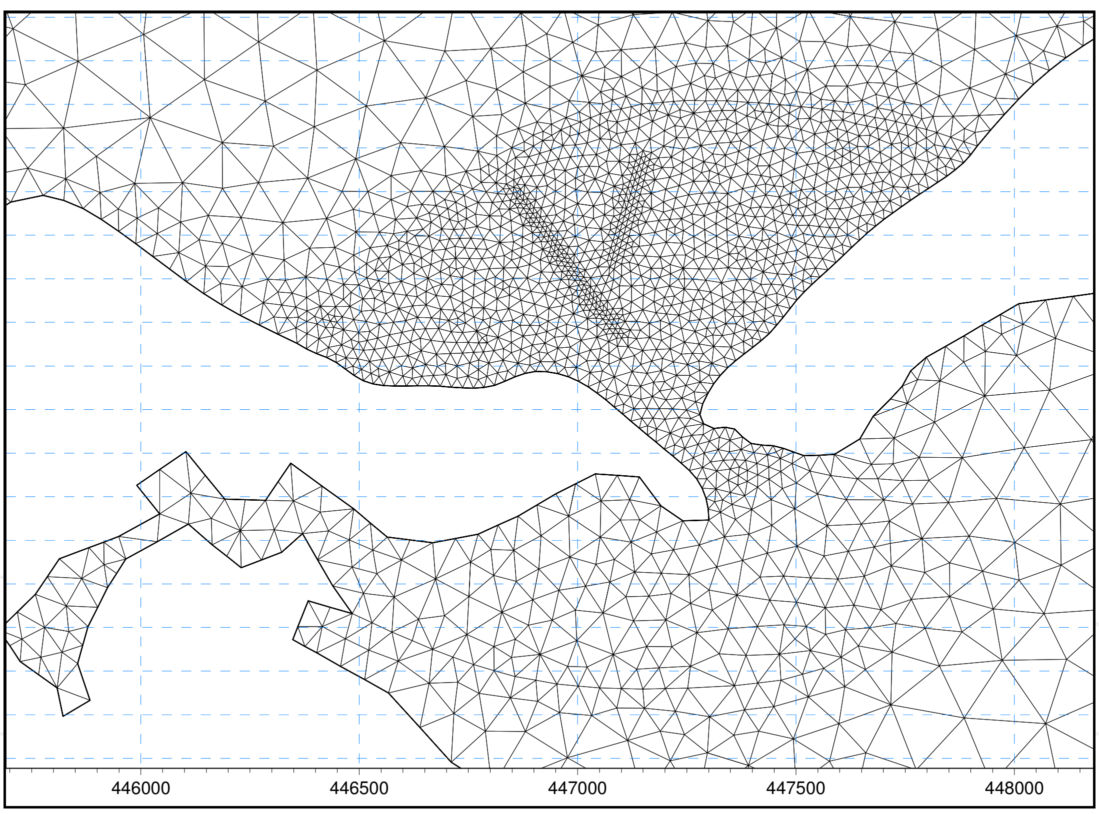


Fig. 14. High-resolution Darnley Inlet model mesh with higher resolution over dredged channels.

The process of ebb dominance on sediment transport at Darnley Inlet is shown on Fig. 15. In effect, during at least 60% of the month, there is one dominant ebb tide per day, meaning that on average, the sand transport direction through the channel is seaward. This is due to the ebb current being above the threshold for incipient sand motion for a longer period of time than the flood current. Sand transported away by the ebb tide deposits off the inlet, forming the ebb shoal.

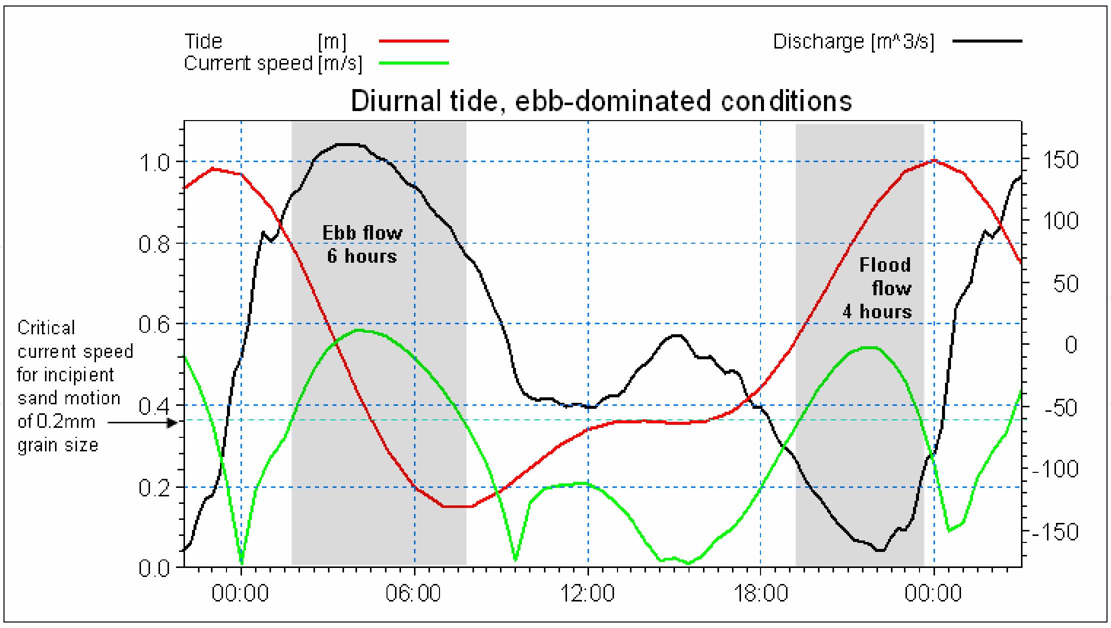


Fig. 15. Time-series of modelled current speed during ebb-dominated conditions

**Wave-driven sediment transport**

Prevailing Northeasterly offshore waves break on a shallow offshore bar (Malpeque Bay's ebb shoal) before reaching the inlet where storm wave heights are controlled by water level. Using spectral wave model MIKE21 SW, it was estimated that significant wave heights incident to the inlet and adjacent spits are less than 1m when the water level is at or below high tide. Northeasterly waves arrive at the East spit at a very oblique angle to the shoreline, causing significant Eastward longshore transport. In contrast, prevailing wave crests arrive near-perpendicular to the West spit shoreline, causing lower longshore sediment transport rates.

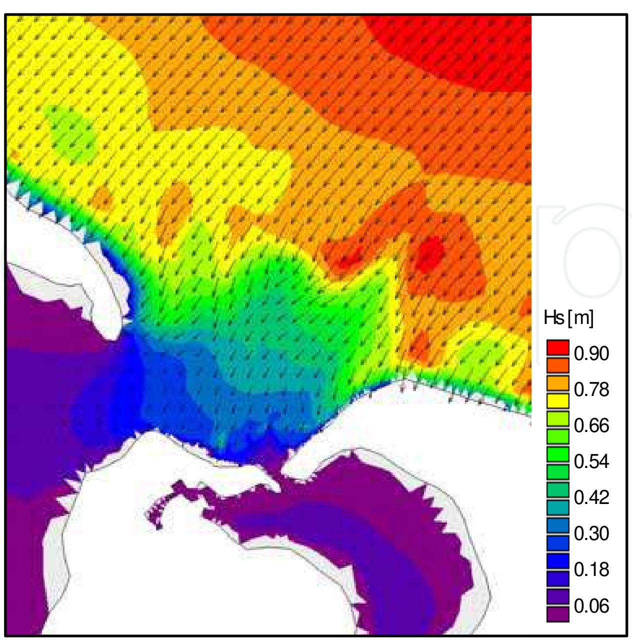


Fig. 16. Modelled near-shore wave height transformation for offshore waves of significant height 1m and peak period 8s.

Potential bulk longshore sediment transport rates were calculated based the standard CERC (1984) formula, using modelled breaking significant wave height parameters along representative shoreline reaches. The results are presented on Fig. 17. As a convention, left- and right-directed longshore transport rates are negative and positive, respectively. The net transport is the sum of left and right-directed transport rates. It is cautioned that:

- The effect of strong, reversing tidal currents from Malpeque Bay is not included; and
- The sediment transport values shown assume infinite sand supply, which is rarely the case. In the long-term, the beach sizes and sand masses are constantly adjusting to gradients in longshore transport rates, which themselves evolve as a function of sand supply and changing shoreline orientation.

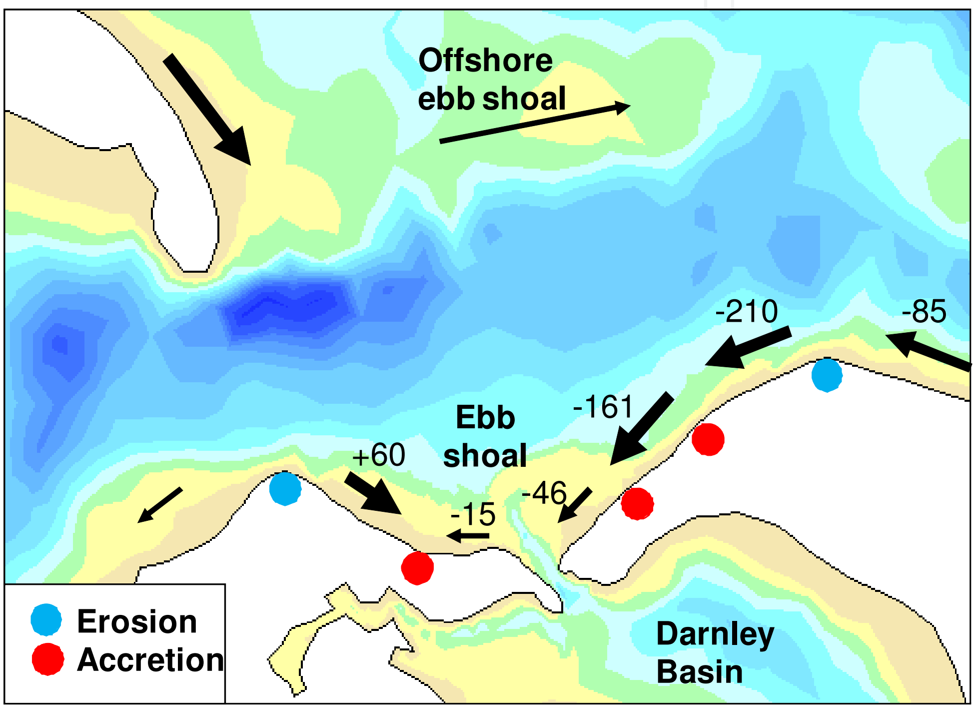


Fig. 17. Net potential longshore sediment transport rate (1000's $m^3$/ year) based on wave forcing. The arrows indicate the direction of net transport. Erosion occurs in areas of increasing transport, while decreasing gradients in longshore transport results in accretion.

Gradients in potential longshore transport rates, caused by changing wave parameters or shoreline orientation, are used to identify areas of shoreline erosion or accretion and to explain observed trends:

- The net transport at the inlet is from East to West; the inlet throat location is therefore likely to continue migrating westward;
- The large differences in potential transport rates between the East and West spits would cause large deposition volumes into and near the inlet, notably at the ebb shoal;
- The growth of the East spit seen on aerial photographs (Fig. 13) can be explained by the along-shore gradient in transport potential due to diminishing wave heights;
- The location of the pre-1960's inlet at the base of the West spit is likely accreting due to converging shorelines on either side. This would have contributed to the original inlet closure; and
- Headlands represent eroding sediment sources.

**Empirical tools for assessing inlet stability**

Despite the complexities of the physical processes, morphologic characteristics of inlets such as cross-sectional area at the throat or ebb shoal dimensions have been successfully correlated to parameters such as tidal prism, wave climate and longshore sediment transport rate. Empirical relationships have been developed by researchers for sandy inlets worldwide, the largest available datasets being from the continental U.S. A review of these predictive tools is provided by Kraus (2008), and those found useful to understanding the sediment dynamics at Darnley Inlet are applied herein.

Inlet stability can refer to either the cross-sectional area of the channel across the inlet throat, or to the inlet location. With respect to the former, since the tidal prism must enter and exit through the relatively constricted inlet, flow increases and sediment is scoured until the inlet erodes to a stable channel cross sectional area. A natural channel is only stable when it is both large enough to allow full tidal passage yet small enough so constricted tidal currents flush the excess sand out. Jarrett (1976) examined the relationship between tidal prism and inlet throat cross sectional area, based on data at 108 inlets. The relationship derived from his data is plotted on Fig. 18.

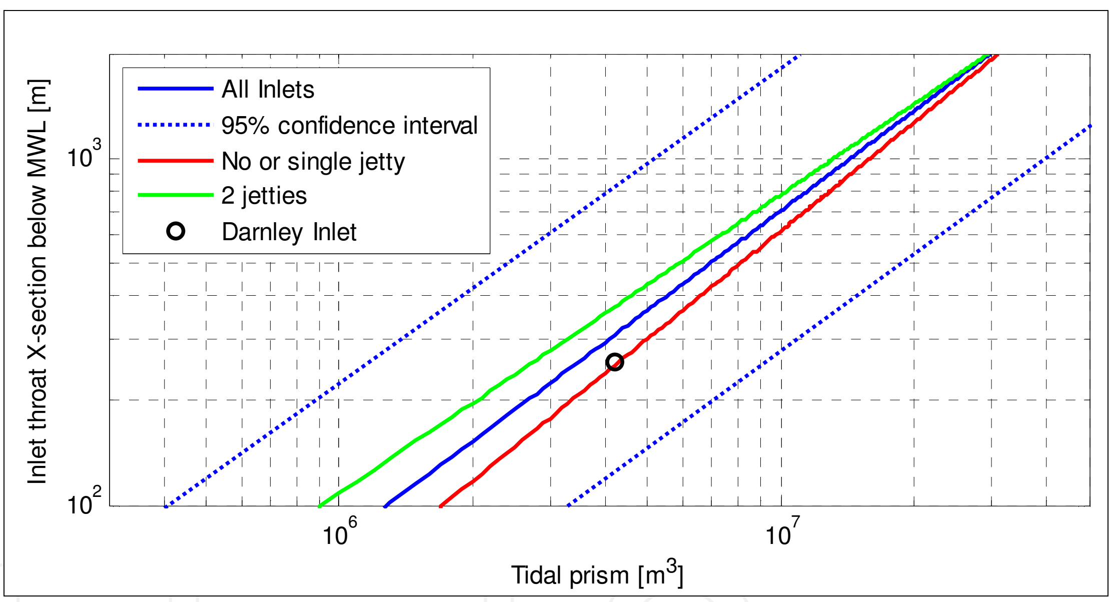


Fig. 18. Empirical equilibrium cross-sectional area at the inlet throat vs. tidal prism (after Jarrett 1976).

Darnley Inlet fits the trend line well, and the 270m² measured cross sectional area is at near-equilibrium dimensions. Jarrett's data suggests that parallel jetties may increase the cross-sectional area by about 40% at the throat (this does not consider channel size over the ebb shoal).

It is useful to predict the consequences of a departure from the equilibrium cross section. The question is whether the inlet would tend to close or scour itself back to its equilibrium shape after a sudden storm-induced deposition reduces the cross section. The analysis procedure was summarized by Dean and Dalrymple (2002), and is referred to as the Escoffier method. The results are graphically presented in Fig. 19. The maximum inlet velocity is calculated based on the Keulegan (1967) equation, accounting for inlet cross-section, upstream area, friction, entrance and exit losses using a semidiurnal tide.

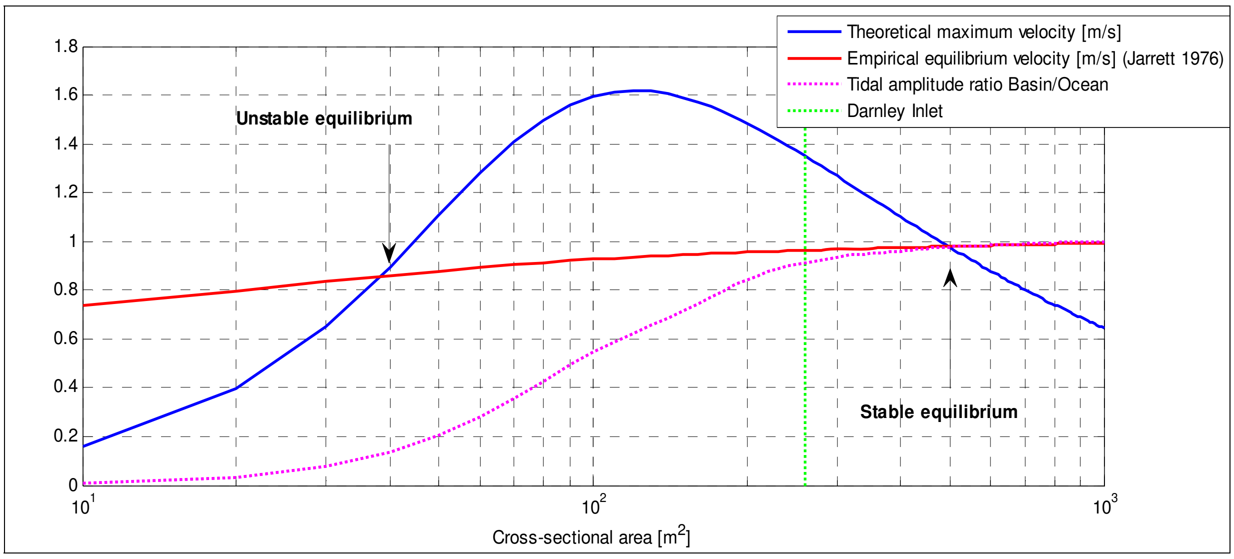


Fig. 19. Maximum and equilibrium inlet velocity vs. throat cross-sectional area.

Small entrance channels that limit tidal passage are dominated by friction, and their equilibrium is unstable. If a storm reduces the cross-section, friction increases, tidal passage decreases and the maximum velocity decreases, leading to more infilling, and ultimate closure of the inlet and relocation of the channel to a more hydraulically efficient location. This illustrates what likely happened at Darnley Inlet in the 1960's. The new inlet through the East spit grew towards stable equilibrium while the original inlet to the West became unstable and eventually closed. When the cross section was wide enough for most of the tide to go through (tidal passage over 70-80%), the influence of friction was much reduced. At stable inlets, storm-induced sedimentation increases maximum velocities by reducing the cross-sectional area, causing he channel to scour back to stable equilibrium. For a cross section of 270m$^2$, the maximum equilibrium velocity through the inlet throat is about 1m/ s, which is consistent with numerical model results and other published estimates of maximum tidal current necessary for inlet channel stability (Kraus 2008). In summary, the tidal prism of Darnley Basin can only support one stable inlet. The inlet cross-section itself appears stable and not at risk of closure.

In terms of the inlet location, longshore sediment transport influences the tendency of un-jettied inlets to migrate along the shore, regardless of dredging schedule. Bruun and Gerritsen (1966) examined the influence of the tidal prism over annual longshore transport ratio P/ Q, arguing that the longshore transport should play a role in inlet stability. In the present case, using P=4.2 10$^6$ m$^3$ (from the MIKE21 model) and Q=46,000 m$^3$/ year, P/ Q is below 100, which means the inlet position is more likely to be unstable and result in shifting channels with significantly large shoals. This conclusion is consistent with observations showing that the inlet throat position is migrating westward. This translation is supported by the strong westward longshore transport, and has been facilitated so far by the relatively lower elevation at the tip of the West spit between its well vegetated dune and the channel. As seen at other shifting tidal inlets, there is a possibility that the East spit overlaps the eroding tip of the West spit. This would create a more angled and less hydraulically efficient channel, compounding the navigational difficulties.

**Morphological modelling**

The DHI MIKE21 Coupled Model was used to investigate engineering alternatives to ebb shoal dredging. The model includes a dynamic coupling between DHI's sand transport model, the aforementioned hydrodynamic module and the spectral wave model MIKE21 SW. Feedback of the bed level changes on the waves and flow calculations is included, as well as dynamic coupling of flow and wave calculations. This model is typically used for investigating the morphologic evolution of the nearshore bathymetry due to the impact of engineering works (coastal structures, dredging works etc.). It is most suitable for short to medium-term investigations (a few weeks) over a limited coastal area. The computational effort becomes impractically large for long-term simulations, or for large areas. Fine sand of median grain size 0.2 mm was assumed throughout the domain based on field samples.

A morphological sediment transport model is ideally calibrated using a series of pre- and post storm bathymetries. However, with this site (as with many others), the temporal resolution of sounding surveys do not allow that level of detail. The model results can still be compared to dredging records for an order-of-magnitude validation. Two runs were carried out to validate the model for existing conditions:

- a 1-month, short-term simulation with varying wave height to investigate the infilling processes at the dredge channel, and
- a medium-term simulation with constant wave activity and using a speedup factor in the bed level changes to artificially accelerate the morphologic evolution. The medium-term simulation setup served as a template for modelling the morphologic effects of engineering alternatives to dredging.

*Short-Term Simulation*

The model was run for a period of 1 month including several representative wave events. Input time-series for the month of October 2004 were imported from an offshore wind and wave hindcast, which included several wave events of various magnitudes. The initial bathymetry included a typical 2m-deep, 20m-wide dredged channel through the ebb shoal.

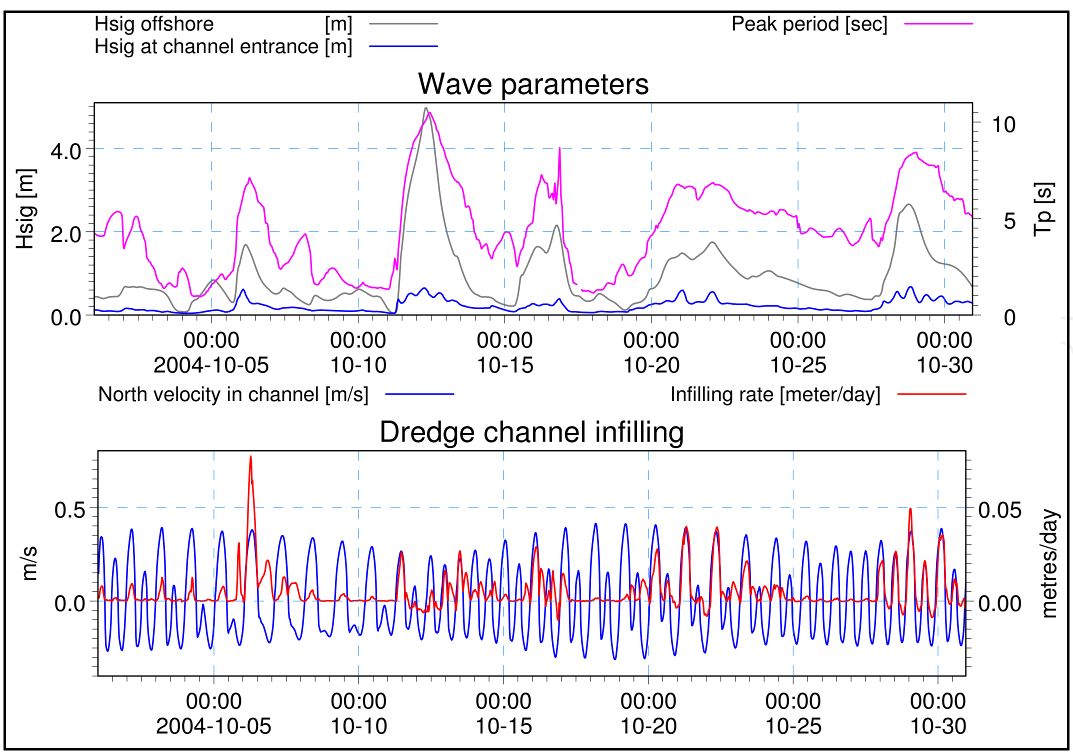


Fig. 20. Time-series of modelled dredge channel infilling rates vs. tidal current and wave parameters.

The mechanisms and occurrence of sedimentation events can be better understood with plots of infilling rates versus current and wave parameters, as shown in Fig. 20. The model indicates that sediment suspension occurs during wave events, and most of the infilling occurs during the ebb tide (on both spring and neap tides) when waves and currents oppose each other. Some channel scouring occasionally occurs, mostly on the flood tide, but only to be overcome by infilling on the next ebb tide. Sediment transport is typically triggered by local waves above 0.3 m, or offshore waves above 0.5 m, which occurs 38% of the year. During these events, the peak infilling rate is typically 0.02 to 0.04 m/ day on the ebb tide, i.e. 0.0035 to 0.0070 m per tide. Based on a 38% yearly occurrence, this translates into an infilling rate of 0.9 to 1.8 m/ year, which is consistent with dredging requirements.

The relatively low wave height threshold that triggers infilling explains why dredging is also required after the summer season. In fact, the waves incident to the inlet ebb shoal are depth limited due to the offshore ebb shoal, therefore the infilling rate is not proportional to the offshore wave height. In simple terms, channel infilling occurs gradually at each moderate wave event and not only during large storms.

Modelled sediment transport loads during a spring tide and a Northeasterly wave event are shown on Fig. 21. Longshore transport patterns along exposed shorelines near the open bounday are primarily wave driven. However, transport within the inlets where waves are depth limited, including Darnley Inlet, is very much influenced by tidal currents. For this particular event, the sediment transport direction varies with tidal currents. These effects add significant uncertainty to the longshore estimates shown on Fig 17. In a qualitative sense the wave-induced differences between left and right directed longshore transport are reduced by tidal currents.

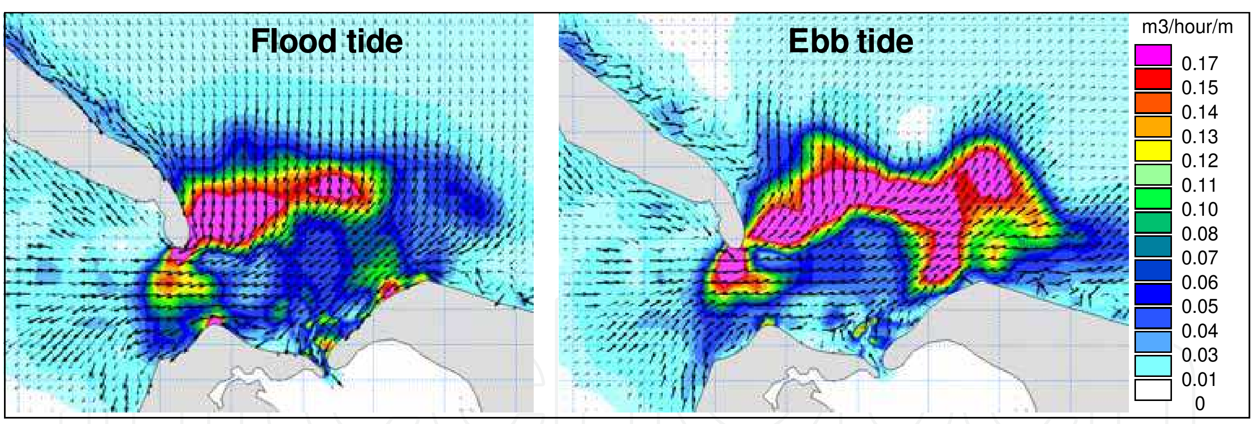


Fig. 21. Modelled sediment transport loads during a northeasterly wave event with significant wave height 1m and peak period 8s.

Long-term simulations (annual to decadal) would yield more accurate longshore transport estimates but would require a much larger computing effort than typically done for preliminary studies. However, medium-term morphologic evolutions can be investigated using artificial parameters to speed up the model, as presented below.

*Medium-Term Morphological Simulation*

Results from the short-term simulation indicated that the offshore significant wave height of 0.5 m was a trigger for sediment transport causing infilling in the dredge channel. To speed up the morphologic evolution in the medium-term simulations, significant wave heights at the offshore boundary were assigned a constant 1m value (the mean height for wave records greater than 0.5m). Assuming a 38% yearly occurrence of such waves, the modelled morphologic changes would occur 1/0.38=2.6 times faster than normal. For increase computational effeciency, a speedup factor of 72 was applied to the rate of bed level change computed every hour (speed up factors must be used cautiously because sudden bed level changes trigger numerical instabilities in the hydrodynamics). The resulting total morphological speedup is difficult to estimate, because the tidal variations cannot be artificially accelerated, and the areas of accelerated erosion versus deposition vary with the tidal stage. In any case, the simulations were stopped when the depth over the ebb shoal had levelled off to a near stable level. The results for existing conditions show that ebb shoal morphologic equilibrium is reached after 16 model days, which in real-time would take 6 months. This suggests that the ideal model speedup factor should be on the order of 10.

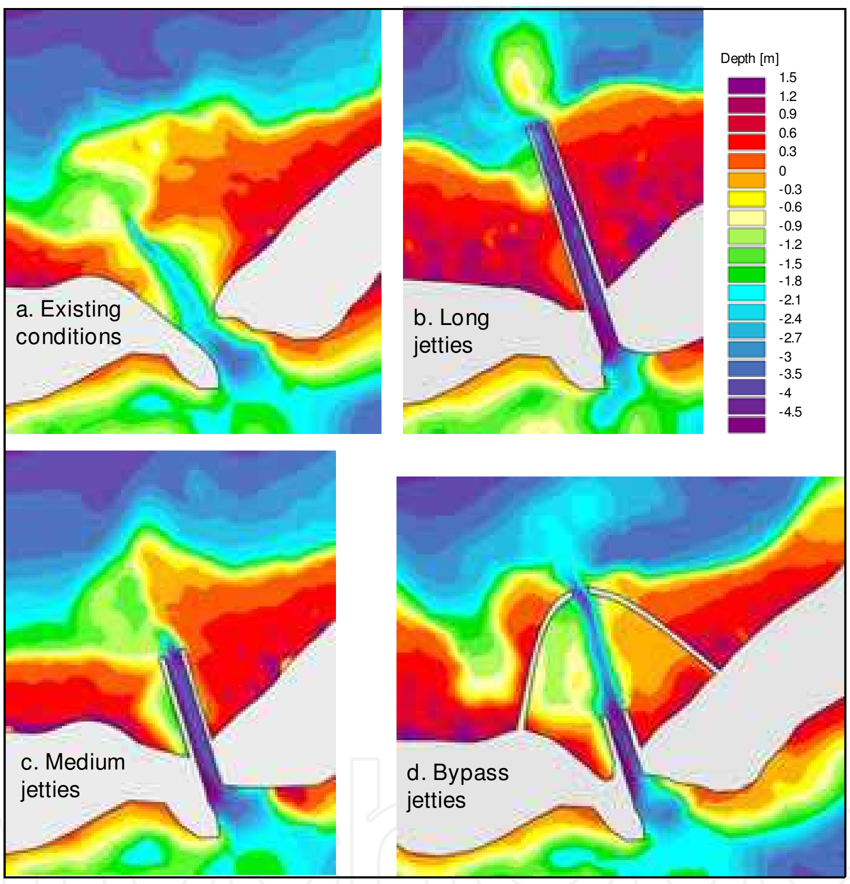


Fig. 22. Modelled morphologic evolution of Darnley Inlet under natural conditions (a) and with jetties of various configurations (b, c, d).

The model was used to investigate the effectiveness of inlet stabilization jetties to improve navigation over the ebb shoal. The bathymetry at the ebb shoal morphologic equilibrium stage for various scenarios is shown on Fig. 22. Inlet engineering presents a conflict between navigational requirements, which can only be met by interrupting longshore transport into the channel, and the necessity of sediment bypassing to ensure shoreline stability. Jetties would have to extend 600m from the inlet throat to provide a significant reduction in dredging costs. Shoreline impacts would include updrift accretion at the East spit and potential downdrift erosion on the West spit, which would be attenuated by transport from the west headland. Shoreline impacts can be mitigated by using curved ‘bypass’ jetties that improve sediment bypassing (details and examples are given by Mangor (2004)). Short jetties may be used to stabilize the inlet location, which is the primary purpose of many jetties at tidal inlets where maintenance dredging is still required. At this site the migrating inlet does not represent an erosion risk to any property or infrastructure, but the structures would help towards a more predictable channel. Short jetties would have a lesser impact on the adjacent shorelines, but would provide no significant reduction in dredging requirements. Finally, it is cautioned that morphologic response to an inlet has a long time-scale and great spatial extent. Long-term processes, such as the migration of the inlet throat under existing conditions, are not represented in the present modelling exercise.

## 4. Conclusion

Coastal sediment transport is of paramount importance for many harbour developments, as it dictates maintenance dredging requirements and shoreline response (erosion and accretion) to coastal structures. A site-specific harbour planning study should provide a thorough understanding of the local environment through various methods, some of which are presented herein. Traditional analysis methods have generally relied upon local experience, aerial photographs, bathymetric and oceanographic surveys, and simple analytical and/ or empirical models. To complement these necessary first steps, advances in numerical models over the last decade make it possible to efficiently assess coastal sediment transport and its implications for infrastructure projects.

Over the next decade coastal morphology will be studied using new and improved modelling tools and techniques. These may include improvements to existing 3D morphological models such as better parameterizations of sediment processes, especially for fine-grained sediments (i.e. flocculation, fluid mud, turbulent interactions), and new methods such as smooth-particle hydrodynamic simulations (a mesh-free particle-tracking method) which depend on high-end computing. The different examples presented in this chapter underline the importance of using a site-specific approach and local observations in the application of numerical models. Improved predicting capabilities for morphologic models are, and will continue to be an important area of future research.

## 5. Acknowledgements

The authors would like to thank Public Works and Government Services Canada and the Small Craft Harbours Branch of the Department of Fisheries and Oceans for providing funding for the studies described herein. Valuable insights given by the Saint John Port Authority and John Hughes Clarke (University of New Brunswick) are also gratefully acknowledged.

## 6. References

Booij, N., R. Ris, and L. Holthuijsen (1999), A third-generation wave model for coastal regions: 1. Model description and validation, *J Geophys. Res.*, 104(4), 7649– 7666.

Bruun, P., and Gerritsen, F. (1959). Natural bypassing of sand at coastal inlets. *J Waterways and Harbors* Div. 85, ASCE, 401-412.

Chen, C, R. C. Beardsley and G. Cowles (2006). An unstructured grid, finite-volume coastal ocean model (FVCOM) system. *Special Issue entitled "Advance in Computational Oceanography", Oceanography*, vol. 19, No. 1, 78-89.

CERC (1984). Shore Protection Manual. Coastal Engineering Research Center, U.S. Army Corps of Engineers, Vicksburg.

Dabees M.A., Kamphuis J.W. (2000). NLINE: Efficient Modeling of 3-D Beach Change. *Proceedings of the 25th International Conference on Coastal Engineering*, Sydney Australia, ASCE pp.2700-2713.

Dean R.G. (2002). Beach Nourishment Theory and Practice. *Advanced Series on Ocean Engineerting* – Vol 18. World Scientific Publishing.

Dean, R.G., and Dalrymple, R.A. (2002). Coastal Processes With Engineering Applications. Cambridge U. Press, 475p

Demirbilek Z., Vijay Panchang V. (1998). CGWAVE: A Coastal Surface Water Wave Model of the Mild Slope Equation. *U.S. Army Corps of Engineers Technical Report CHL-98-xx*

DHI Software (2009). MIKE, Coastal Hydraulics and Oceanography – User Guide. Danish Hydraulic Institute.

DHI Software (2008). LITPACK -An integrated modeling system for littoral processes and coastal kinetics – User Guide. Danish Hydraulic Institute.

Forbes, Donald L, George S. Parks, Gavin K. Manson and Lorne A Ketch, 2004. Storms and Shoreline Retreat in the Southern Gulf of St. Lawrence. *Marine Geology 210* (pp 169-204).

Gravens, M., Kraus, N. and Hanson, H. (1991). GENESIS: Generalized Model for Simulating Shoreline Change – *Report 1: Technical Reference, Technical Report CERC-89-19*, U.S. Army Waterways Experiment Station, Coastal Engineering Research Center, Vicksburg, MS.

Greenberg, D.A. (1990). The Contribution of Modelling to Understanding the Dynamics of the Bay of Fundy and Gulf of Maine. *Modeling Marine Systems*, Vol. 2, A.M. Davies, ed., CRC Press, Boca Raton., Fla., 107-140.

Jarrett, J.T. (1976). Tidal Prism-Inlet Area Relationships. *GITI Report 3*, U.S. Army Waterways Experiment Station, Vicksburg, MS.

Keulegan G.H. (1967). Tidal Flow in Entrances. U.S. Army Corps of Engineers, Committee on Tidal Hydraulics, Tech. Bull. 14, Vicksburg.

Kraus, N. C. (2008). Engineering of Tidal Inlets and Morphologic Consequences. In: Kim Y. (editor). *Handbook of Coastal Engineering*. World Scientific Press. Singapore, in press. 39p.

Lesser, G., J. Roelvink, J. van Kester, and G. Stelling (2004), Development and validation of a three-dimensional morphological model, *Coastal Eng*, 51, 883-915.

Leys, V. (2007). 3D Flow and Sediment Transport Modelling at the Reversing Falls – Saint John Harbour, New Brunswick. *Proceedings of MTS/IEEE Oceans Conference*, Vancouver BC, Canada, Sep 29-Oct 4 2007.

Mangor, K. (2004). Shoreline Management Guidelines. Published by DHI Water and Environment, Horsholm, Denmark.

McCulloch M. M., Forbes D.R., Shaw R.W and A041 Scientific Team. 2002. Coastal Impacts of Climate Change and Sea Level Rise on Prince Edward Island. Geological Survey of Canada. Open File 4261.

Neu, H. A. (1960). Hydrographic survey of Saint John Harbour, NB. National Research council of Canada, Mechanical Engineering Report MH-97.

Pelnard-Considere, R. (1956). Essai de Theorie de l'Evolution des Formes de Rivages en Plage de Sable et de Galets. *Fourth Journees de l'Hydralique, les Energies de la Mer*, Question III, Rapport No. 1, pp. 289–298

Shchepetkin, A.F. and J.C. McWilliams (2005). The Regional Ocean Modeling System (ROMS): A split-explicit, free-surface, topography-following coordinates ocean model, *Ocean Modelling*, 9, 347-404.

U.S. Army Corps of Engineers (2004). Status of Current Hopper and Bin Measurement Technologies. *Technical Note ERDC TN-DOER-T6*. September 2004.

Warner, J.C., Sherwood, C.R., Signell, R.P., Harris, C.K. and Arango, H.G. (2008). Development of a three-dimensional, regional, coupled wave, current, and sediment transport model. *Computers and Geosciences*, 34, 1284-1306.

Winterwerp, J. C. (2005). Reducing harbor siltation. I: Methodology. *J Waterway, Port, Coastal and Ocean Engineering*. Vol. 131, No. 6, Nov 2005, pp. 258-266

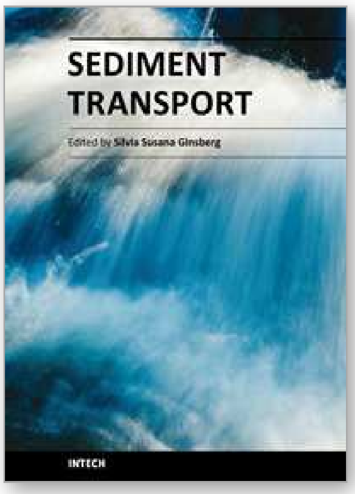


**Sediment Transport**

Edited by Dr. Silvia Susana Ginsberg

ISBN 978-953-307-189-3
Hard cover, 334 pages
**Publisher** InTech
**Published online** 26, April, 2011
**Published in print edition** April, 2011



**InTech Europe**
University Campus STeP Ri
Slavka Krautzeka 83/A
51000 Rijeka, Croatia
Phone: +385 (51) 770 447
Fax: +385 (51) 686 166
www.intechopen.com

**InTech China**
Unit 405, Office Block, Hotel Equatorial Shanghai
No.65, Yan An Road (West), Shanghai, 200040, China
中国上海市延安西路65号上海国际贵都大饭店办公楼405单元
Phone: +86-21-62489820
Fax: +86-21-62489821